BRILL

JOURNAL OF CRUSTACEAN BIOLOGY, 32(5), 802-815, 2012

Journal of Crustacean Biology

PROTEOGLYCAN OCCURRENCE IN GASTROLITH OF THE CRAYFISH *CHERAX QUADRICARINATUS* (MALACOSTRACA: DECAPODA)

María S. Fernández [1,*], Cristián Bustos [1], Gilles Luquet [2], Daniel Saez [1], Andrónico Neira-Carrillo [1], Marion Corneillat [3], Gérard Alcaraz [3], and José L. Arias [1]

[1] Faculty of Veterinary Science, University of Chile, Santiago, Chile
[2] Biogéosciences, UMR CNRS 6282, Université de Bourgogne, 6 Bd. Gabriel, 21000 Dijon, France
[3] UPSP PROXISS, Département Agronomie Environnement, AgroSupDijon, Dijon, France

ABSTRACT

Biomineralized structures are hybrid composites formed and stabilized by the close interaction of the organic and the inorganic phases. Crayfish are good models for studying biomineralization because they develop, in a molting-mineralization cycle, semi-spherical mineralized structures referred to as gastroliths. The organic matrix of these structures consists of proteins, polysaccharides, and lipids. Chitin is the main polysaccharide and is concentrically arranged as fibrous chitin-protein lamellar structures. Although several proteins and low-molecular weight phosphorylated components have been reported to be involved in gastrolith mineralization, the occurrence and role of proteoglycans have not been fully documented. We have immunologically analyzed the proteoglycans in gastrolith matrix extracts and histological cross-sections of the gastrolith, and the forming epithelium during premolt and postmolt stages. The results indicate that gastroliths contain proteoglycans that have dermatan-, chondroitin-4- and 6-, and keratan sulfate glycosaminoglycans. These macromolecules are closely associated with the mineral phase of the gastrolith and are easily removed by decalcification procedures. There is also evidence to indicate that epithelial secretion of some of these molecules is temporally regulated during the molting cycle. However, the precise role of these macromolecules in the calcification and stabilization of the amorphous calcium carbonate phase of the gastrolith remains to be established.

KEY WORDS: amorphous calcium carbonate, biomineralization, calcium storage, *Cherax*, gastrolith, glycosaminoglycans, proteoglycans

DOI: 10.1163/193724012X649804

INTRODUCTION

Biomineralization is a widespread phenomenon in nature leading to the formation of a variety of solid biominerals by living organisms, such as intracellular crystals in prokaryotes, exoskeletons in protozoa, algae, and invertebrates, spicules, lenses, bones, teeth, statoliths, otoliths, eggshells, plant mineral structures, and also pathological biominerals such as gallstones, kidney stones, and oyster pearls (Lowenstam and Weiner, 1989; Mann et al., 1989, 2007; Simkiss and Wilbur, 1989; Bauerlein, 2000, 2007; Mann, 2001; Arias and Fernández, 2007; Arias et al., 2007).

These biologically produced biominerals are inorganic-organic hybrid composites formed by self-assembled bottom up processes under mild conditions, where the small amount of organic component not only reinforces the mechanical properties of the resulting composite but exerts a crucial control on the mineralization process by contributing to the determination of the size, crystal morphology, specific crystallographic orientation, and remarkable properties of the particles formed (Belcher et al., 1996; Falini et al., 1996; Weiner and Addadi, 1997; Nys et al., 1999; Smith et al., 1999). Therefore, understanding biological routes for the structuring of biomaterials is becoming a valuable approach for the synthesis of novel materials (Arias et al., 2004).

Because of the significant calcium turnover that occurs in their metabolism, Crustacea represents one of the most remarkable phyla in which to study such a biomineralization process. Among crustaceans some species cyclically elaborate calcium storage structures (Luquet and Marin, 2004). For example, crayfish develop a pair of semi-spherical mineralized structures referred to as gastroliths. They are formed in the anterior lateral wall of the cardiac stomach between the epidermis and the cuticle in a place known as the gastrolith disc. Gastrolith development occurs during the premolt stage when the innermost part of the exoskeleton is resorbed. During gastrolith formation, histomorphological and histochemical changes are observed in the gastrolith disc tissue (Travis, 1963). Notably the epidermal cells show a high concentration of acid mucopolysaccharides followed by a decrease upon completion of the gastrolith. Gastroliths are resorbed during postmolt stage (Luquet and Marin, 2004).

The organic matrix of these structures consists of proteins, polysaccharides, and lipids (Travis, 1963). Most of the crustacean skeleton and calcified structures (gastrolith included) polysaccharides are in the form of alpha chitin, while barnacle and mollusc shells contain beta chitin (Lowenstam and Weiner, 1989). Gastrolith chitin is concentrically arranged

* Corresponding author; e-mail: sofernan@uchile.cl

as fibrous chitin-protein lamellae (Travis, 1960; Luquet and Marin, 2004; Shechter et al., 2008a).

Although chitin occurs in many calcium carbonate-based biominerals, its role is almost passive in the process of biomineralization (Erhlich, 2010). In fact, it has been demonstrated that neither chitin nor chitosan per se modify in vitro calcium carbonate nucleation and growth (Neira-Carrillo et al., 2005; Diaz-Dosque et al., 2008). However, in many calcium carbonate biomineralized structures, chitin is not present as a single component, but exists together with chitin-associated proteins and possibly polyanionic polysaccharides to form an insoluble three-dimensional scaffolding wherein crystallization is controlled in a confined space (Arias and Fernández, 2003, 2007, 2008; Arias et al., 2004).

Proteoglycans are glycoconjugates consisting of a protein core to which linear polysaccharide side chains are covalently attached. These polysaccharides, referred to as glycosaminoglycans, are of variable length and are highly negatively charged. Glycosaminoglycans are alternating copolymers of hexosamine and either galactose or alduronic acid. Individual glycosaminoglycans differ from each other by the type of hexose or alduronic acid, the position and configuration of the glycosidic linkages, and the degree and pattern of sulfation (Casu, 1985; Iozzo, 1998; Huckerby, 2002; Sugahara and Kitagawa, 2002; Bülow and Hobert, 2006; Arias and Fernández, 2008). The major sulfated glycosaminoglycans are keratan sulfate, chondroitin-4- or 6-sulfate, dermatan sulfate, and heparan sulfate (Arias et al., 2004).

The occurrence of proteoglycans in crustacean calcifications has not been fully documented. However, it has been shown that the barnacle shell has a precise distribution of specific proteoglycans (Fernández et al., 2002; Arias and Fernández, 2003) Barnacle shell is built as concentric mineralized layers where a keratan sulfate proteoglycan is located in close association with an inert chitin lamina. Growth of calcite crystals occurs in a gel phase, in which chondroitin-6-sulfate and dermatan sulfate proteoglycans are found (Rodríguez-Navarro et al., 2006). On the other hand, it is to notice that in some calcified biominerals such as crustacean calcium storage structures, the major mineral is amorphous calcium carbonate, the stabilization of which remains unclear (Addadi et al., 2003; Luquet and Marin, 2004; Shechter et al., 2008a).

Proteoglycans are underestimated components of biomineralization (Arias and Fernández, 2008), and their role in the formation of the gastrolith remains unexplored.

In this study we have immunologically analyzed the occurrence of some proteoglycans in gastrolith matrix extracts as well as their immunohistochemical localization in cross-sections of the epithelium that forms the gastrolith and in the gastrolith itself during premolt and postmolt stages.

Materials and Methods

Animal and Sample Preparation

The freshwater crayfish, *Cherax quadricarinatus* von Martens, 1868, were reared in a farm of the Faculty of Veterinary and Animal Sciences, University of Chile, Santiago (Project FIA COO-1-DA. 13). Dorso-ventral radiographs of crayfish specimens were obtained with a General Electric Mobile 225 equipment, operating at 44 kV, 100 mA and 0.08 sec.

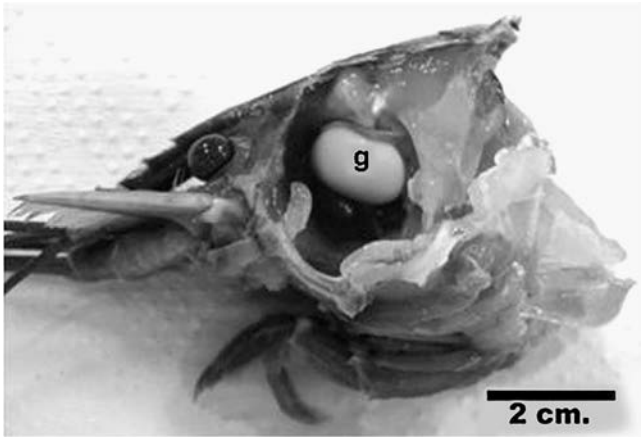

Fig. 1. *Cherax quadricarinatus* head with a fully developed gastrolith inside the stomach. g: gastrolith.

All radiographs were made using Kodak TMG Hyper Speed Green film placed in a 24 × 30 cassette with automatic developing.

For scanning electron microscopy (SEM), sugar analysis and detection of proteoglycans from matrix extracts, gastroliths were extracted at the ecdysis period when the animal sheds its old exoskeleton (Fig. 1). After extraction, gastroliths were incubated in 10% (v/v) NaOCl overnight to remove superficial organic contaminants and then thoroughly rinsed with distilled water. After drying, they were gently ground into powder using an agate mortar and pestle.

For microscopic immunodetection experiments, specimens were first selected at different periods of their molting cycle after radiographic analysis to assess the presence and level of development of the gastroliths according to Nakatsuji et al. (2000). After dissection, three molt stages were selected, early premolt, premolt, and postmolt. Stomachs with corresponding gastrolith from the selected specimens were extracted and treated for histological and immunohistochemical observations.

SEM Analysis

For SEM observation, fully developed gastroliths were slightly broken in a mortar and pestle. While some pieces were observed without any further treatment, others were decalcified with 1 M EDTA for 2 min for a slight surface decalcification. For a more intensive decalcification, pieces were incubated 30 min in 10% acetic acid. Then, after rinsing with distilled water and air-drying, the gastrolith samples were carbon covered and examined with a JEOL 6400 F scanning electron microscope.

Sugar Analysis

Fully developed gastrolith powder was decalcified during 48 hours in cold 10% acetic acid at 4°C. The solution was then centrifuged 30 min at 3893 *g* at 4°C. The pellet, corresponding to the acetic acid-insoluble matrix (AIM), was rinsed 10× with 50 ml MilliQ water (Millipore®), freeze-dried and weighed. The supernatant containing the acetic acid-soluble matrix (ASM) was filtered (5 μm cut-off) and concentrated with an Amicon ultrafiltration system on a Millipore® membrane (YM10; 10-kDa cut-off). The solution (around 5 mL) was extensively dialyzed against

MilliQ water (3 days, several water changes) before being freeze-dried and weighed.

Lyophilized matrix samples were hydrolyzed in 2 M trifluoroacetic acid (TFA) at 105°C for 4 hours. Samples were evaporated to dryness before being resuspended with NaOH (20 mM). The acidic, neutral, and amino sugar contents of the hydrolysates were determined by high-performance anion exchange-pulsed amperometric detection (HPAE-PAD) by using a CarboPac PA100 column (Dionex P/N043055), according to the Dionex instructions. Non-hydrolyzed samples were analyzed similarly, in order to detect free monosaccharides in the samples. Blank experiments were performed using BSA diluted in 10% acetic acid and submitted to all the steps of the extraction procedure. Note that this technique does not allow the quantification of sialic acids, which are destroyed during hydrolysis with TFA.

Primary Antibodies for Immunohistochemistry and Dot Blot

The monoclonal antibodies used for this study were produced and characterized by Bruce Caterson and co-workers against specific epitopes present in proteoglycan substructures located in the sulfated glycosaminoglycans, either in saturated disaccharides or in the unsaturated disaccharides that are produced after digestion with specific endoglycosidic enzymes (Caterson et al., 1987). These antibodies do not cross-react with proteins or other saccharide epitopes. These antibodies are defined as follows:

2B6 (IgG, ICN Biomedical Inc.): This mouse monoclonal antibody specifically binds to the unsaturated disaccharide produced after digestion of dermatan sulfate or chondroitin-4-sulfate by chondroitinase ABC (EC 4.2.2.4) or after digestion of chondroitin-4-sulfate by chondroitinase ACII (EC 4.2.2.5) (Caterson et al., 1985, 1987).

3B3 (IgM, ICN Biomedical Inc.): This mouse monoclonal antibody recognizes chondroitin-6-sulfate after digestion with chondroitinase ABC (EC 4.2.2.4) or chondroitinase ACII (EC 4.2.2.5) (Caterson et al., 1985).

5D4 (IgG, ICN Biomedical Inc.): This mouse monoclonal antibody recognizes a hypersulfated hexasaccharide of keratan sulfate (Mehmet et al., 1986).

Histological and Immunohistochemical Preparations

Stomachs from specimens at different molting stages were fixed in 2% paraformaldehyde, 0.2% glutaraldehyde in 200 mM phosphate buffered saline solution (PBS), pH 7.4 for 48 hours. Then samples were washed in PBS, decalcified for 48 hours in Ana Morse decalcification solution containing 10% formic acid and 5% citric acid (Morse, 1945) mixed 1:1 with fixative solution, then changed to a 2:1 proportion for another 48 hours and another change to a 4:1 proportion for an additional 48 hours. Finally, samples were washed three times with PBS, dehydrated in ethanol, embedded in paraffin, and processed using routine histological techniques in order to obtain serial sections of the stomachs.

Paraffin sections were processed for hematoxylin-eosin (H-E) staining and for immunohistochemistry using monoclonal antibodies against specific glycosaminoglycans (Caterson et al., 1985, 1987). Sections were enzymatically treated with chondroitinase ABC or ACII when needed. Horseradish peroxidase (HRP)-conjugated rabbit anti-mouse Ig (Mouse/Rabbit Polyscan Kit, HRP-DAB Detection System, Cell Marque) was used as secondary antibody.

As primary antibodies, we used 2B6 to detect both dermatan sulphate, and chondroitin-4-sulfate, 3B3 to detect chondroitin-6-sulfate, and 5D4 to detect keratan sulfate. All of the primary antibodies were diluted 1:100 in 1% BSA in PBS (BSA/PBS). For 2B6 and 3B3, the sections were treated with chondroitinase ABC prior to the primary antibody incubation. Chondroitinase ABC treatment generates the unsaturated structure in chondroitin sulfate and dermatan sulfate that is necessary for 3B3 and 2B6 reactivity.

Briefly, sections were hydrated in PBS for 10 minutes and then, for 2B6 or 3B3, sections were treated with 0.1 IU/mL chondroitinase ABC for one hour at 37°C. All the sections were treated with 3% hydrogen peroxide in methanol for 15 minutes to block endogenous peroxidase activity and then incubated in 3% BSA/PBS for 15 minutes to block nonspecific sites. Sections were incubated overnight at 4°C in the respective primary antibodies. After three washes in PBS, sections were incubated with the secondary antibody at room temperature for 45 minutes, washed with PBS, and finally incubated with diaminobenzidine chromogen for 10 minutes at room temperature. Sections were then washed with distilled water and covered using a hydrophilic mounting medium. The intensity of the reaction is different for each primary antibody under equivalent conditions. Therefore, comparison of reaction intensity only can be done for the same antibody in different samples. In each experiment, negative controls were done by incubating sections only with the secondary antibody. As an additional negative control, sections not treated with chondroitinases and then incubated only with the secondary antibody were done. Images at two different magnifications were included to better show the relationship between the gastrolith and the epithelium that synthesizes it. The same samples were observed under fluorescence microscopy to detect chitin autofluorescence.

Proteoglycan Detection by Dot Blot

Powdered fully developed gastroliths were decalcified in 10% formic acid at 4°C. The solution obtained, containing the whole organic matrix, was then extensively dialyzed against bidistilled water in 3500 MWCO membrane tubing (Spectra/Por, Spectrum Lab., CA). Two fractions were obtained by centrifugation (1500× *g* for 20 minutes at 4°C): the supernatant corresponding to the soluble fraction and the pellet which represents the insoluble fraction. Both fractions were separately lyophilized and separately processed to prepare two proteoglycan-enriched fractions (Yanagishita and Hascall, 1984; Arias et al., 1992; Carrino et al., 1994, 1997).

Briefly, each of the lyophilized samples was solubilized in a solution of 4 M guanidinium chloride, 0.05 M sodium acetate, pH 5.8. The samples were chromatographed on Sephadex G-50 (Pharmacia) columns eluted with 8 M urea, 0.15 M sodium chloride, 0.5% CHAPS, 0.05 M sodium acetate, pH 6.0, and the V_0 material was loaded onto a DEAE-Sephacel column that was equilibrated in the same solution. Proteoglycans are negatively charged molecules, which adsorb to DEAE-Sephacel. After the column was rinsed with loading buffer to remove the tissue proteins, the proteoglycans were eluted in a stepwise fashion with 0.25 M and then

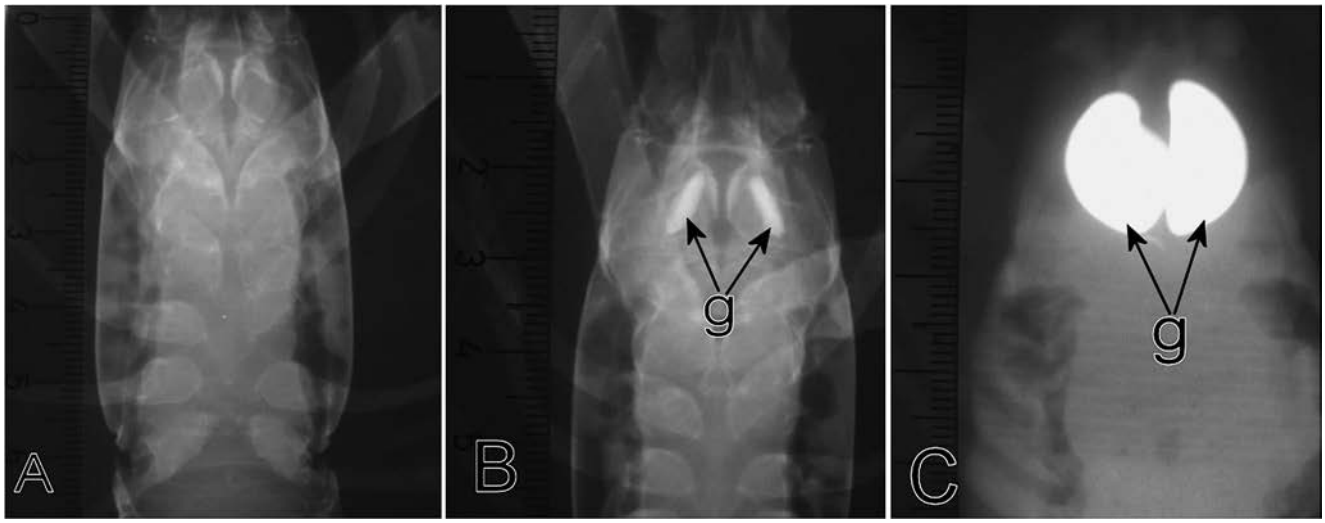

Fig. 2. Radiographic view of early premolt (A), premolt (B) and early postmolt stages (C) crayfish cephalothorax. A, absence of radiopaque structure at level of stomach; B, presence of radiopaque structures corresponding to forming gastroliths; C, well-defined radiopaque structures corresponding to fully developed gastroliths.

1.0 M sodium chloride, both in 8 M urea, 0.5% CHAPS, 0.05 M sodium acetate, pH 6.0. The concentration of proteoglycans in the DEAE pools of the gastrolith soluble or insoluble fractions was determined by the Safranin O assay (Carrino et al., 1991). The isolated proteoglycans were analyzed by dot blot with monoclonal antibodies (Carrino et al., 1991). For the dot blots, equal amounts of proteoglycans were loaded for the proteoglycans isolated from the soluble and insoluble fractions. The samples were dot blotted with a Bio-Dot microfiltration apparatus (Bio-Rad, Richmond, CA). Samples in TBS were blotted onto nitrocellulose membrane (Bio-Rad), and the membranes blocked with 3% BSA in TBS-Tween (TBS with 0.05% Tween 20). Membranes were then enzymatically treated with chondroitinase ABC or ACII when needed, i.e., for 2B6 and 3B3. Membranes were incubated with a primary antibody diluted 1:1000 in 3% bovine serum albumin (BSA) in TBS-Tween. After washing 3 times in TBS-Tween, the membranes were incubated with a secondary antibody, alkaline phosphatase-conjugated goat anti-mouse (Promega), which was diluted 1:7500 in TBS-Tween. After washing again in TBS-Tween, the membranes were then incubated in alkaline phosphatase substrate solution, nitrotetrazolium blue and 5-bromo-4-chloro-3-indolyl phosphate in alkaline phosphatase buffer (0.1 M sodium chloride, 5 mM magnesium chloride, 0.1 M Tris, pH 9.5). Rinsing the membranes with distilled water stopped the color development. The membranes were then air-dried. TBS was used as a negative control (−C) and cartilage proteoglycans from bovine nasal septum as a positive control (+C).

RESULTS

Radiographic Analysis

By radiographic observation, three molt stages were selected depending on the presence or absence in the stomach of radiopaque structures corresponding to gastroliths. The stage that we could designate intermolt due to the absence of a radiopaque structure (Fig. 2A) according to the determination of Nakatsuji et al. (2000) better corresponds, after observing serial sections of the stomach, to an early premolt stage because of the presence of a gastrolith disc but without appreciable calcification. In premolt stage, well defined radiopaque structures were found (Fig. 2B) corresponding to gastroliths in formation, and in animals selected as being in early postmolt by direct observation of a previous ecdysis, huge well defined radiopaque structures, corresponding to fully developed gastroliths, were observed in the stomach lumen (Fig. 2C).

SEM Analysis of Gastrolith Structure

Fully developed gastroliths, at ecdysis, are cup-shaped structures showing an outer convex side in contact with the stomach epithelium, which synthesizes the gastrolith, and an inner concave side facing the stomach lumen (Fig. 3A). In cross-section, after slight decalcification they show a dense structure of successive concentric layers, as well as cross striations (Fig. 3B). It is possible to sequentially decalcify the gastroliths, and after 72 hours in formic acid or acetic acid, only organic fibers remain. Figure 3C shows large-diameter fibers probably corresponding to chitin-protein fibers forming a basic 3-dimensional framework of organic matrix. The pocket-like structures thus elaborated, within which calcium carbonate is precipitated, are probably themselves subdivided by fibers of nanometric diameters as observed by SEM at higher magnification (Fig. 3D).

Histological Analysis

Sections of early premolt stage showed the initial formation of a gastrolith (Fig. 4A and B). At this stage the gastrolith disc epithelium, the cuticle, and the initial gastrolith can be distinguished. The gastrolith is in close association with the gastrolith disc formed by cuboidal cells of the epithelium. The cuticle covers the luminal side of the gastrolith in formation, and the newest and oldest parts of the gastrolith can be

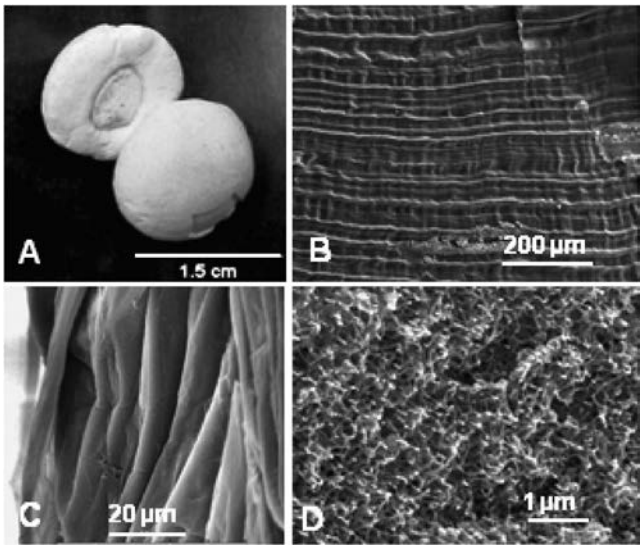

Fig. 3. Structure of a gastrolith. A, general aspect of paired gastroliths of *Cherax quadricarinatus*; B, gastrolith cross-section after partial decalcification with EDTA showing layered pattern; C, SEM view of organic matrix layers remaining after complete decalcification; D, organic matrix fibers of nanometric diameter after 30 min decalcification with acetic acid.

distinguished by their differential staining by hematoxylin-eosin. The reason of such difference remains unclear.

At premolt stage, larger gastroliths were found. The gastrolith disc epithelium consists of higher cylindrical cells, and it is still in close association with the forming gastrolith (Fig. 4C). The lamellar structure of the gastrolith can be distinguished (Fig. 4D). As in the early premolt stage, a differential staining by hematoxylin-eosin was observed between the newest and the oldest parts of the gastrolith, and the cuticle, as at the previous stage, covers the luminal surface of the gastrolith.

At postmolt stage, sections showed a very large but disorganized gel-like gastrolith in the stomach lumen. Some of the gastrolith disc epithelium and part of the cuticle still remained attached to the gastrolith (Fig. 4E and F).

A layered structural organization of autofluorescent chitin is observed in early premolt and premolt gastroliths, while it is almost completely lost at the postmolt stage revealing the disorganization of the chitin-protein fibril network concomitant with the physiological decalcification process (Fig. 5A to C).

Sugar Analysis of Gastrolith Matrix

The amounts of the different monosaccharides detected by chromatographic analysis after TFA hydrolysis are reported in Table 1 and classified by order of abundance for the acetic acid insoluble fraction. The insoluble matrix fraction (IM) exhibits a high level of glucosamine, around 75% of the total sugar content, whereas the soluble matrix fraction (SM) exhibits 35% glucosamine, which is also the most important sugar in this fraction. Nevertheless, the order of abundance of the other sugars varies considerably in the 2 matrices, with xylose, arabinose and glucose being the most important (around 7.4, 6 and 4.7% respectively) in the IM matrix *versus* glucose, fucose and mannose in the SM each one representing more that 10% of the total sugar content (around 14, 12.7 and 10.5% respectively). It is to notice that iduronic acid, component of dermatan sulfate, cannot be detected by this method.

Immunohistochemical Analysis

To facilitate visual comparisons, the same negative immunohistochemical controls have been repeated in figures A and B of the next three figures (Figs. 6 to 8).

Compared to control sections treated only with secondary antibody (Fig. 6A and B), sections treated with 2B6 antibody showed a dermatan sulfate and chondroitin-4-sulfate reactivity in early premolt and premolt stages with a positive reaction in the gastrolith disc epithelium closely associated with the forming gastrolith (Fig. 6C to F), and in the gastrolith itself in the early premolt stage (Fig. 6C and E). At the early premolt stage, a more intense reaction was observed in the newest part of the gastrolith (Fig. 6C and E). However, the gastrolith labeling is negative during the premolt stage (Fig. 6D and F).

Compared to control sections treated only with secondary antibody (Fig. 7A and B), sections treated with 5D4 antibody showed a strong positive reaction for keratan sulfate in the gastrolith disc epithelium and in the gastrolith at the early premolt stage (Fig. 7C-E), while at the premolt stage the reactivity in the gastrolith and in the gastrolith disc epithelium is almost absent (Fig. 7D-F).

When sections treated with 3B3 antibody (Fig. 8C to F) were compared with control sections treated only with secondary antibody (Fig. 8A and B), a chondroitin-6-sulfate positive reaction was found at the early premolt stage, in the gastrolith and in the gastrolith disc epithelium (Fig. 8C and E). At the premolt stage, there is only a very weak 3B3 reactivity in both the epithelium and the gastrolith (Fig. 8D and F).

At postmolt stage, when sections treated with 2B6, 5D4, and 3B3 antibodies (Fig. 9B to D respectively) were compared with control sections treated only with secondary antibody (Fig. 9A), a weak positive reaction to dermatan sulphate, chondroitin-4-sulfate and chondroitin-6-sulfate was found only in the gastrolith disc epithelium but it was negative in the formic acid decalcified gastrolith remnant (Fig. 9B and D). At this stage, a negative reaction to keratan sulfate was observed in both, the gastrolith disc epithelium and the resorptive gastrolith remnant (Fig. 9C).

Proteoglycan Detection by Dot Blot

Proteoglycans were isolated from the soluble and insoluble fractions of 10 (25 g) decalcified fully developed gastroliths and then analyzed. The concentration of proteoglycans was measured at 6.4 μg/μl in the soluble fraction and 13.3 μg/μl in the insoluble fraction, giving a total amount of 640 ng of proteoglycans per mg of gastrolith organic matter. Proteoglycans from the soluble fraction showed a positive reaction for all the antibodies used, and the reaction was especially intense for chondroitin-4-sulfate when it is compared with that of the insoluble fraction (Fig. 10). Proteoglycans from the insoluble fraction showed an intense reaction for dermatan sulfate plus chondroitin-4-sulfate and for chondroitin-6-sulfate, while the keratan sulfate reaction was negative compared with the standard sample of bovine nasal septum (Fig. 10). It is important to remember that quantitative comparisons should only be

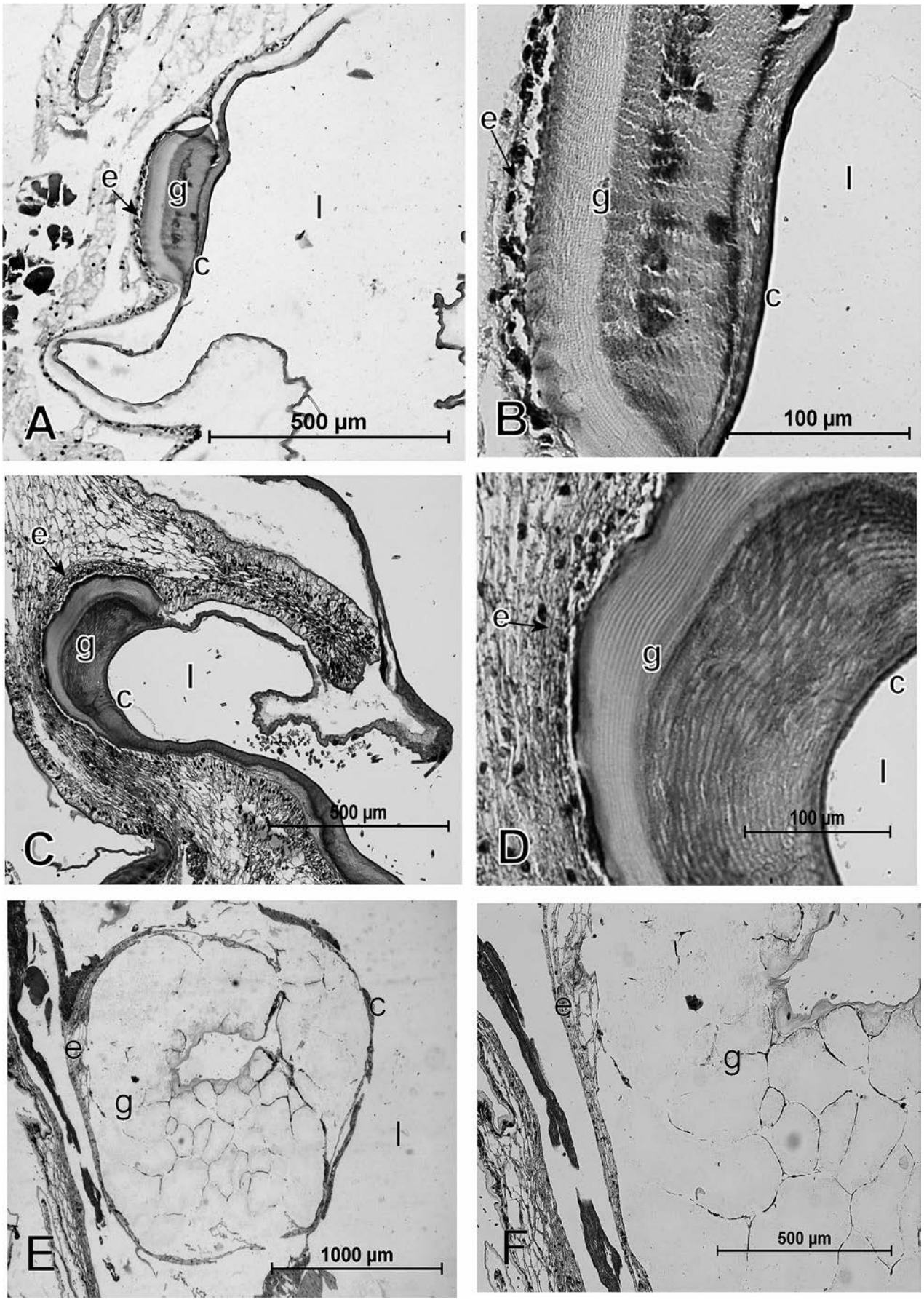
A
e
g
c
l
500 µm
B
e
g
l
c
100 µm
C
e
g
c
l
500 µm
D
e
g
c
l
100 µm
E
c
e
g
l
1000 µm
F
e
g
500 µm

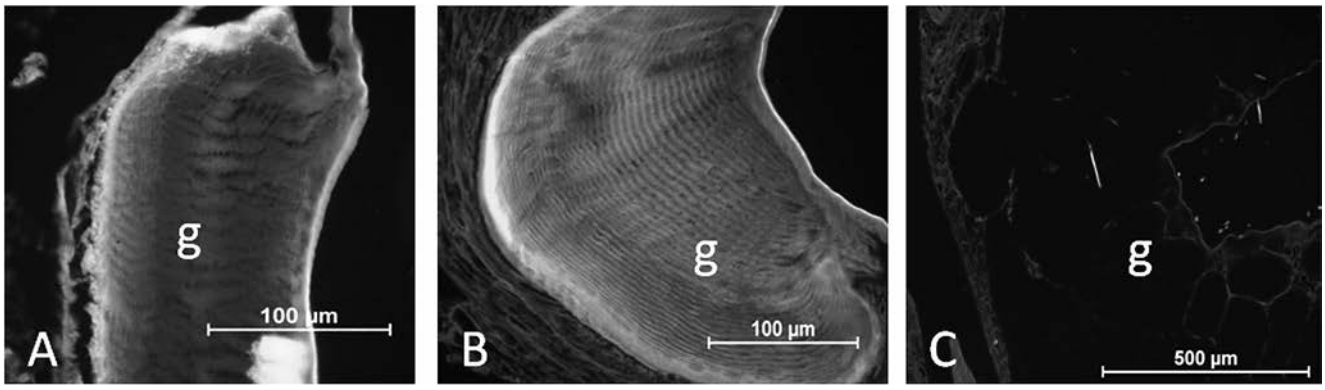

Fig. 5. Autofluorescence of chitin in gastrolith cross-sections at three stages of development. A, early premolt; B, premolt; and C, postmolt. Chitin organized as multilayered structure at early premolt and premolt stages and disorganized after decalcification at postmolt stage.

done between reactivities of different samples to the same antibody because of the difference in the sensitivity of each antibody against its own antigen.

Discussion

Various organisms use amorphous calcium carbonate (ACC) as a temporary storage form for calcium and carbonate ions (Lowenstam and Weiner, 1989; Aizenberg et al., 2002; Luquet and Marin, 2004; Gago-Duport et al., 2008). This can occur because ACC is the most unstable polymorph of calcium carbonate and can be easily dissolved in aqueous and acidic environments. However, biogenic ACC can be stabilized for a long period of time by components of the organic matrix, demonstrating that organisms are also able to inhibit crystallization.

Although the exact mechanism by which ACC is stabilized *in vivo* requires further investigation, it is known that stabilization of ACC has been commonly achieved by using various additives, including magnesium and phosphate ions, phosphoamino acids (Raz et al., 2000; Loste et al., 2003; Ajikumar et al., 2005; Lee et al., 2005; Bentov et al., 2010), biomacromolecules (Aizenberg et al., 1996, 2002; Addadi et al., 2003; Shechter et al., 2008b; Glazer et al., 2010), and synthetic polymers (Volkmer et al., 2005; Xu et al., 2005).

In some crustaceans, such as lobsters, terrestrial crabs, and crayfish, transient semi-spherical calcium storage structures, called gastroliths, are cyclically elaborated in the stomach wall in relation with the cyclic renewal of their hard exoskeleton (calcified cuticle) for growing. The ability of crustaceans to stabilize ACC in these transient calcium storage structures is remarkable (Raz et al., 2002; Addadi et al., 2003; Becker et al., 2003; Luquet and Marin, 2004), but what kind of macromolecules are involved in the stabilization of ACC or crystalline phases has not been well established. Even stabilized, biogenic ACC remains highly soluble, which is beneficial for the subsequent use of the ions to partially calcify each new carapace (Raz et al., 2002).

Several proteins characterized from crustacean transient calcium storage structures, such as orchestin (Testeniere et al., 2002), gastrolith matrix protein (GAMP) (Ishii et al., 1996; Tsutsui et al., 1999; Tagaki et al., 2000), GAP 65 (Shechter et al., 2008b), and GAP 10 (Glazer et al., 2010), have been shown to be involved in their calcification. But only GAP 65 has been associated with the stabilization of ACC during gastrolith formation. More recently, the presence of phosphorylated energy-rich intermediates of the glycolytic pathway as components of the gastrolith organic matrix has been reported and their possible involvement in the formation and stabilization odf ACC suggested (Akiva-Tal et al., 2011; Sato et al., 2011).

Although, different types of components have been characterized in various calcium storage deposits in invertebrates, little is known about the occurrence of proteoglycans in these structures. Proteoglycans are known to be components of calcium carbonate biomineralized structures (Arias

Table 1. Amounts of the different monosaccharides detected by chromatographic analysis after TFA hydrolysis.

Sugar	*Cherax* matrix analyzed	
	IM	SM
Glucosamine	72.42 ± 2.36	35.85 ± 0.35
Xylose	7.44 ± 0.52	3.15 ± 0.64
Arabinose	6.12 ± 0.56	1 ± 1.41
Glucose	4.7 ± 0.37	13.95 ± 5.44
Mannose	3.74 ± 0.75	10.45 ± 2.05
Fucose	3.42 ± 1.19	12.65 ± 0.35
Galactose	1.14 ± 0.50	8.4 ± 2.55
Galactosamine	1.02 ± 0.42	5.65 ± 2.19
Rhamnose	Tr	8.3 ± 0.71
Galacturonic acid	Tr	Tr
Glucuronic acid	Tr	Tr

Tr, trace.

Fig. 4. Histological sections of stomach tissue stained with hematoxylin-eosin (H-E). A and B, development of gastrolith (g) in close association with gastrolith disc epithelium (e) during early premolt stage, cuticle (c) covers the luminal side of forming gastrolith, difference in staining seen between oldest part (dark) and newest part (pale) of gastrolith; C and D, gastrolith (g) in formation during premolt stage, epithelium (e) tightly linked to forming side of gastrolith (g), also showing differential staining seen between oldest and newest parts of gastrolith, cuticle covering gastrolith clearly visible (c); E and F, disorganized decalcified gastrolith during postmolt stage.

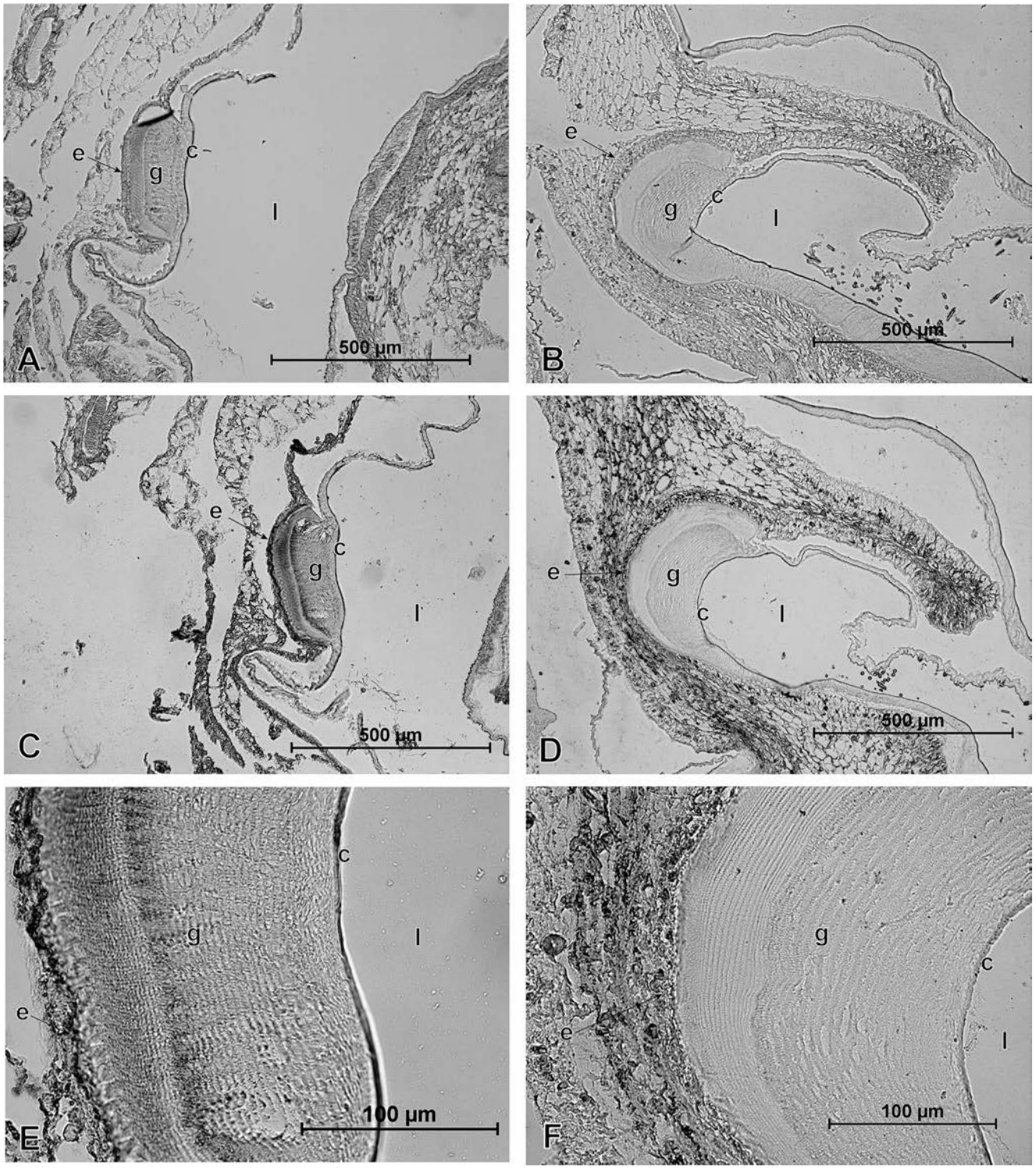

Fig. 6. 2B6 immunohistochemistry of early premolt (A, C and E) and premolt (B, D and F) stomach sections. A and B, control; C, D, E and F, 2B6 immunoreactivity. Dermatan sulfate and chondroitin-4-sulfate reactivity visible in gastrolith disc epithelium at both stages and in gastrolith itself in early premolt stage; a positive reaction in connective tissue underlying epithelium also observed.

and Fernández, 2008), but the precise role of such components in diverse aspects of the biomineralization process is not well known.

Although we did not use the molt mineralization indices (Shechter et al., 2008a) to monitor the progress of the molt cycle, we showed here that after radiographic analysis, only premolt and postmolt gastroliths could be detected. When a radiopaque structure was not detected, the crayfish was primary classified as intermolt. However, after a detailed dissection of some of these specimens a small but well

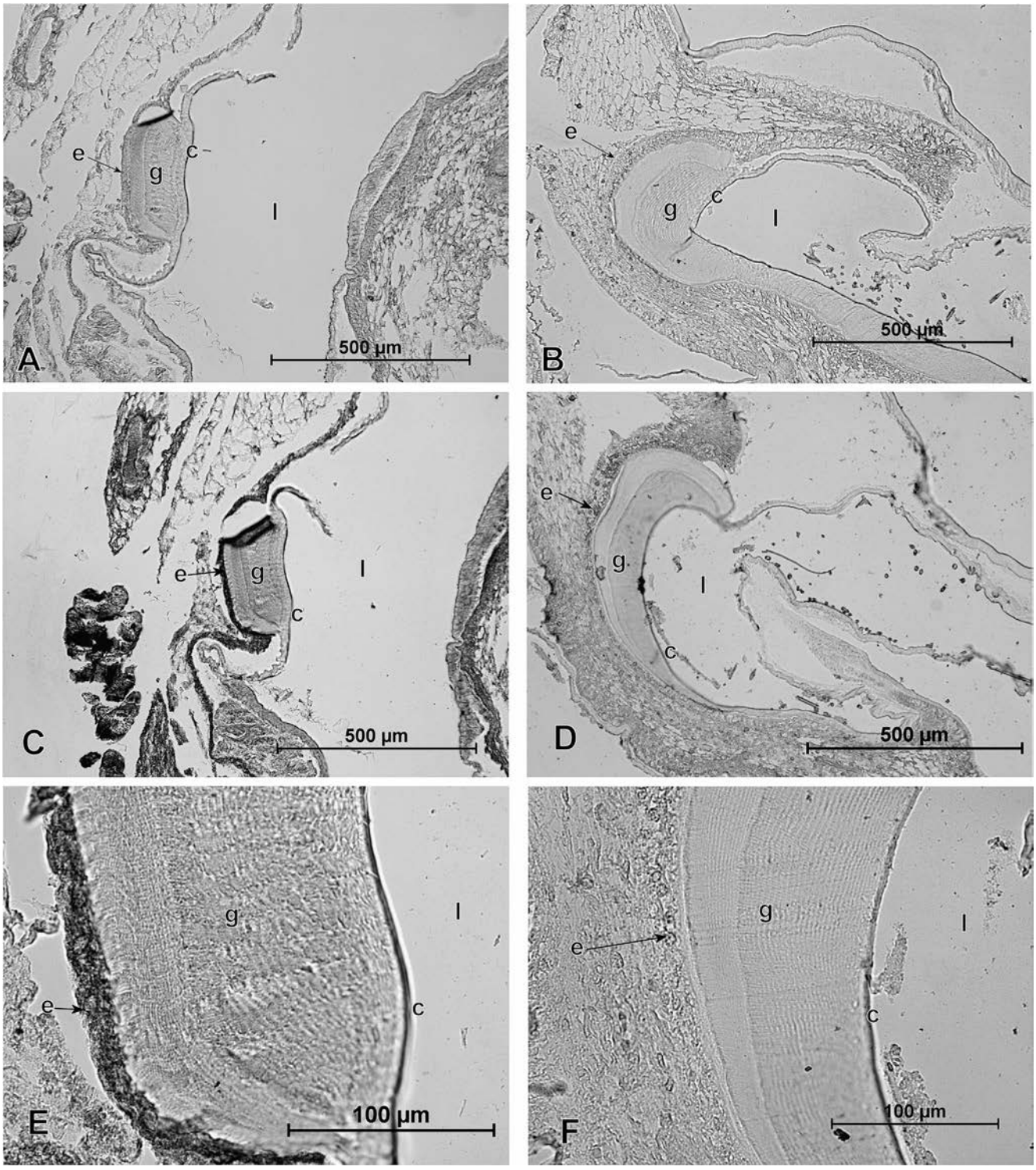

Fig. 7. 5D4 immunohistochemistry of early premolt (A, C and E) and premolt (B, D and F) stomach sections. A and B, control; C, D, E and F, 5D4 immunoreactivity. Keratan sulfate-positive reaction detected in gastrolith (g) and more strongly in gastrolith disc epithelium (e) at early premolt stage (C and E). At premolt stage reactivity almost absent in both gastrolith and gastrolith disc epithelium (D and F).

defined and soft gastrolith was found. These specimens were then reclassified as early premolt stage, meaning that the calcification level of these samples was not sufficient to block the penetration of X-rays in order to produce a radiopaque structure. Therefore, a well defined extracellular matrix, chitin-rich layered structure is formed early, and it subsequently becomes calcified.

The organic matrix of gastrolith is composed of a complex network of chitin-protein fibers forming concentric and transversal striations well visible in a cross-section of a

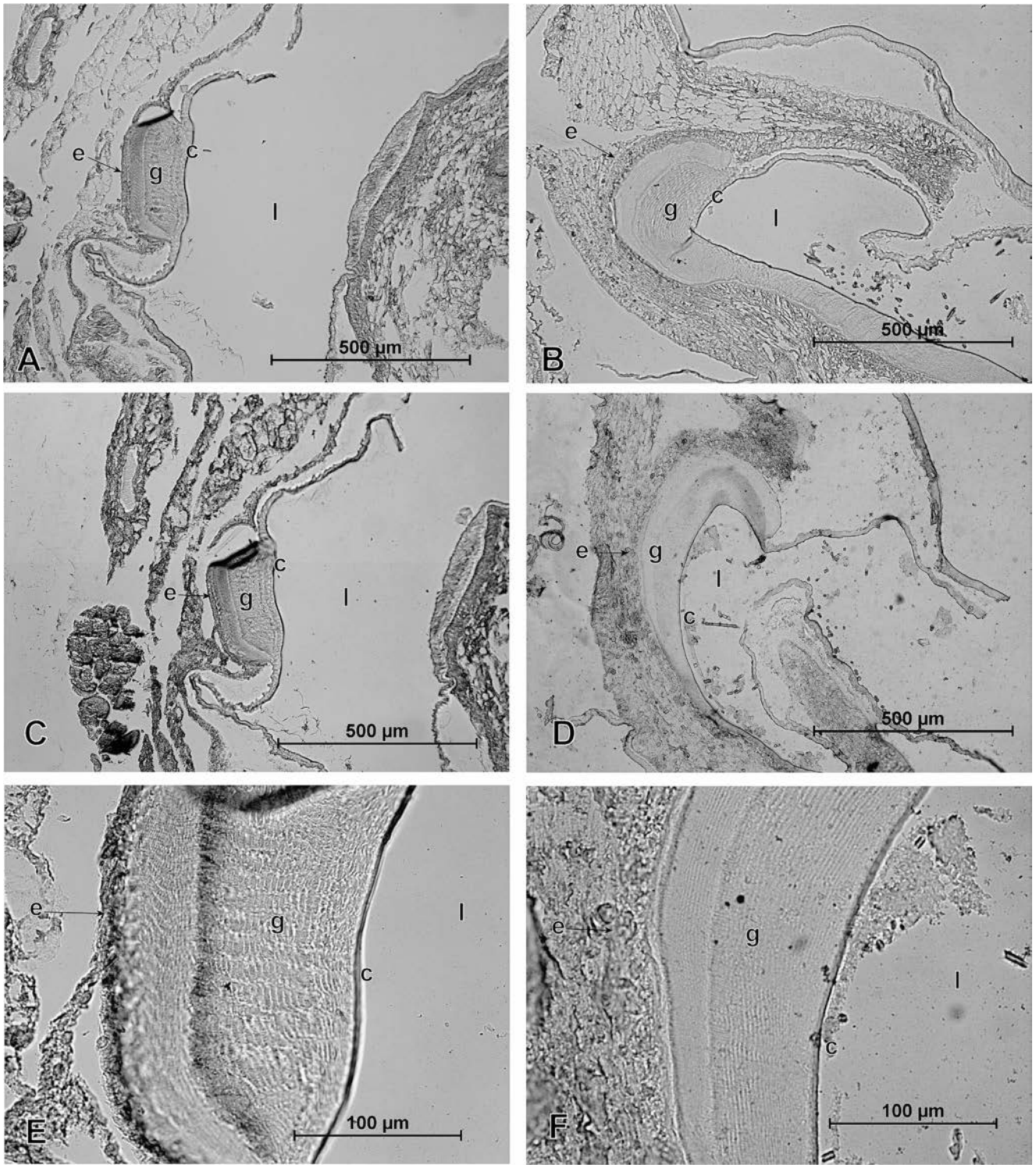

Fig. 8. 3B3 immunohistochemistry of early premolt (A, C and E) and premolt (B, D and F) stomach sections. A and B, controls; C, D, E and F, 3B3 immunoreactivity. Reactivity to 3B3 observed during early premolt at level of gastrolith matrix (g) and gastrolith epithelium (e) (C and E). Very weak reactivity observed in gastrolith and gastrolith disc epithelium during premolt (D and F). Connective tissue, below the epithelium, appears more strongly reactive.

partially decalcified gastrolith. Chitin is a polymer of N-acetylglucosamine, therefore it is not surprising to find a high level of glucosamine in the insoluble fraction. This is in accordance with the presence of large chitin fibers, which cannot be solubilized and depolymerized during the decalcification process. The glucosamine level remains not negligible in the soluble fraction because of the presence of protein-chitin fibers of nanometric diameter which could subdivide

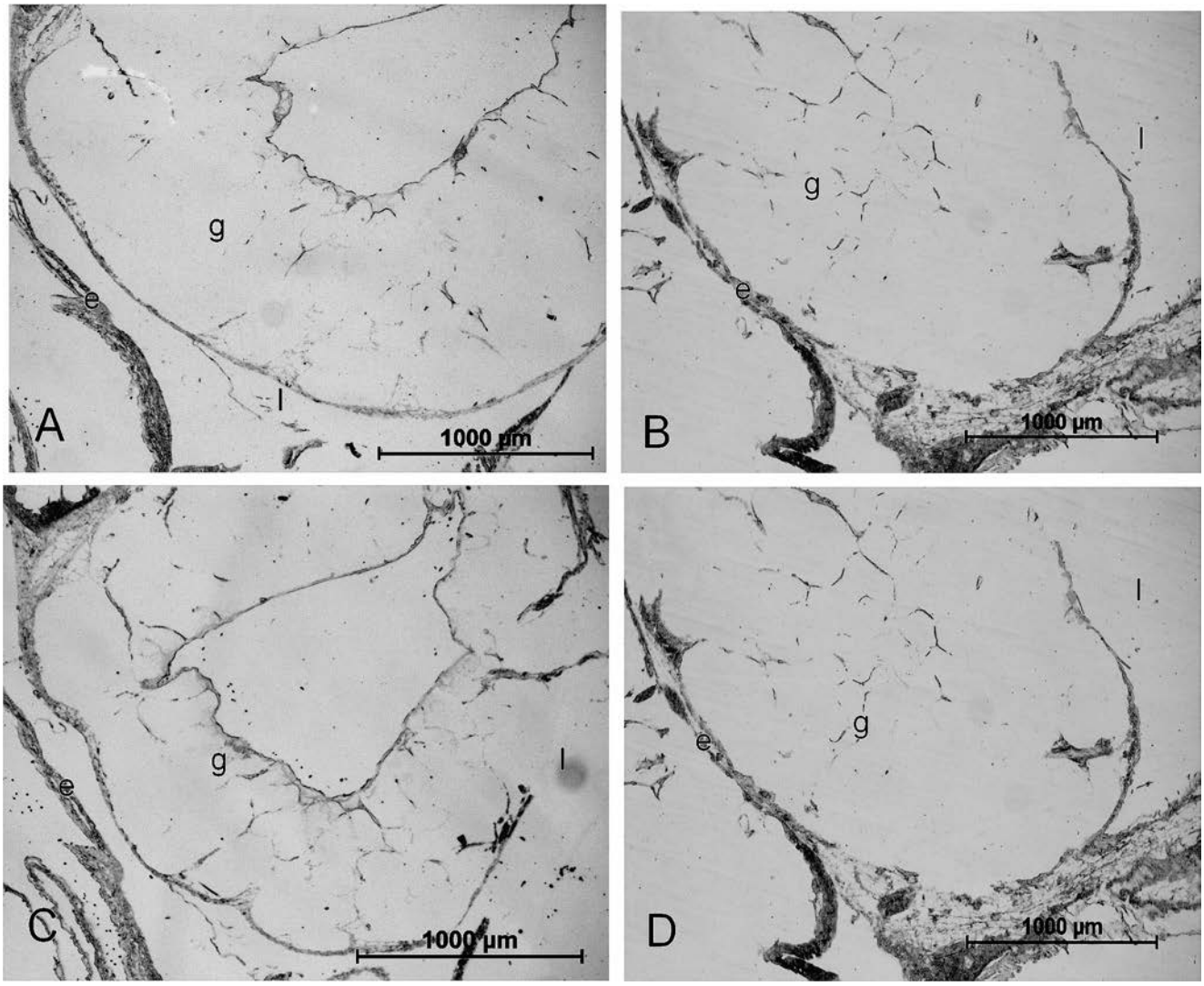

Fig. 9. 2B6, 5D4 and 3B3 immunohistochemistry of postmolt stage. A, control; B, 2B6 immunoreactivity; C, 5D4 immunoreactivity; D, 3B3 immunoreactivity. Weak positive reaction to dermatan sulphate, chondroitin-4-sulfate, and chondroitin-6-sulfate found only in gastrolith disc epithelium, but negative in resorptive gastrolith remnant (B and D). Negative reaction to keratan sulfate observed in both gastrolith disc epithelium and resorptive gastrolith remnant (9 C).

in micro-units the largest pocket-like compartments framed by the micro-chitin fibers. These nanofibers could be released during the decalcification process and could remain in the supernatant after centrifugation of the decalcified solution.

The presence to a lesser extent of other monosaccharides cannot be really explained for all of them like arabinose, fucose or rhamnose. Nevertheless the presence of galactose, galactosamine as well as xylose and mannose can be related to the presence of proteoglycans as others components of the organic matrix. Indeed, chondroitin sulfate, dermatan sulfate and keratan sulfate are proteoglycans composed of a glycosaminoglycan (GAG) bound to a protein core (at the level of a serine or a threonine) *via* a xylose sugar: . . . XY-XY-XY-XY-β(1-3)-Gal-β(1-3)-Gal-β(1-4)-Xyl-β(1-O)-Ser/Thr-Protein. Keratan sulfate (KSII) consists of a glycosaminoglycan (GAG) bound to a protein core (at the level of an Asn) *via* a mannose sugar: . . . carbohydrate chain-Man-β(1-O)-Asn-Protein (Funderburgh, 2000; Arias and Fernández, 2008). The high levels of glucosamine reported here are consistent with the abundance of chitin in the gastrolith, while the low levels of glucuronic acid not necessarily should match the levels of galactosamine containing proteoglycans since dermatan sulfate contains iduronic acid instead of glucuronic acid which was not detected by the method of sugar analysis used.

Immunodetection of proteoglycans on histological sections showed that in the early premolt soft gastrolith, the four glycosaminoglycans studied (dermatan, chondroitin-4- and 6-, and keratan sulfate) are detected both in the gastrolith-forming epithelium and especially in the newest and less calcified region of the gastrolith matrix. However, during the premolt stage when calcification is already detected by X-rays, not all glycosaminoglycans are detected in the gastrolith, and some of them are also absent from the gastrolith-forming epithelium. In early premolt and premolt

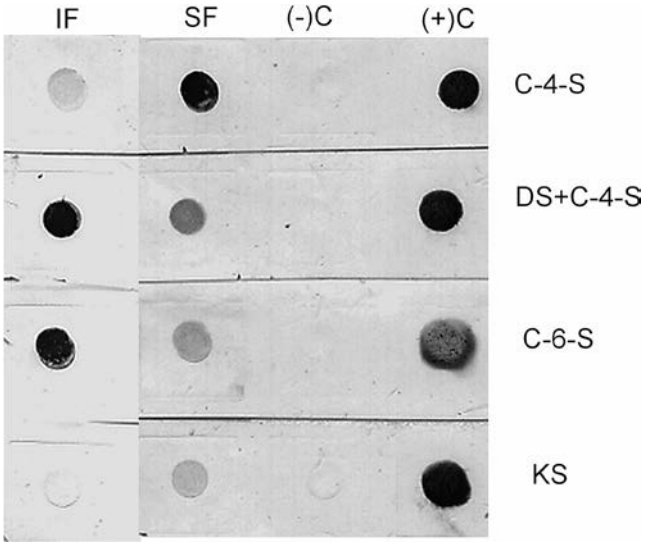

Fig. 10. Dot blot analysis of proteoglycans isolated from soluble (SF) and insoluble (IF) fractions of gastrolith. TBS negative control (−C) and bovine nasal septum proteoglycans positive control (+C). Soluble fraction showed positive reaction for all antibodies used, especially intense for chondroitin-4-sulfate when compared with that of insoluble fraction. Insoluble fraction showed intense reaction for dermatan sulfate plus chondroitin-4-sulfate and for chondroitin-6-sulfate, while keratan sulfate reaction negative compared with standard sample of bovine nasal septum.

gastroliths, the chitin layered structure is still intact, while in the postmolt stage the layered organization is almost completely lost.

When a specific methodology to obtain proteoglycans is applied to a fully formed gastrolith, the same family of glycosaminoglycans reported to occur in other calcium carbonate mineralized systems (Arias and Fernández, 2008) is also found in the red claw crayfish gastrolith. Some of them appeared to be more associated with the insoluble organic fraction while others with the soluble one, which is consistent with what has been shown in other mineralized systems (Fernández et al., 2001; Arias and Fernández, 2003, 2008; Arias et al., 2004).

One plausible explanation for the apparent contradiction between dot blot and immunohistochemical results may be related to the decalcification procedure. In other calcified structures, a very close association has been described between the molecules involved in the process of biomineralization and the crystalline or amorphous mineral phase, where a phase stabilization role has been proposed (Aizenberg et al., 1995, 1996; Albeck et al., 1996; Raz et al., 2002; Bentov et al., 2010; Glazer et al., 2010; Ndao et al., 2010). It is well known that amorphous calcium carbonate-based structures are more soluble and more easily decalcified than the crystalline forms of these biominerals. At the early premolt stage, where the gastrolith is at the beginning of its calcification, the proteoglycans associated with the rest of the extracellular matrix molecules, such as chitin, are not removed by the formic acid-based decalcification solution. However, at the premolt stage when the gastrolith is fully calcified, the decalcification procedure could remove a significant amount of the chitin-associated organic material due to its interaction with $CaCO_3$, as has been recently showed in parallel studies (Thormann et al., 2012). At the postmolt stage there is no detection of proteoglycans, because the gastrolith has been almost totally digested and disorganized with the drastic decalcification procedure used in our studies. As expected, the decalcification procedure does not affect the detection of proteoglycans in the epithelial tissue, and when they are not detected in the epithelium it could be related to a spatio-temporal regulation mechanism such as that reported by Yudkovski et al. (2010) in crayfish or Fernández et al. (1997, 2001) in the eggshell.

The fact that for SF the dot for C-4-S is more intense than the dot for DS + C-4-S, although both of these contain equal amounts of material, is unexpected. The C-4-S dot was treated with chondroitinase ACII to digest chondroitin sulfate. The DS + C-4-S dot was treated with chondroitinase ABC to digest both chondroitin sulfate and dermatan sulfate. Both dots were analyzed with antibody 2B6, which should detect terminal unsaturated disaccharides containing 4-sulfation. These disaccharides should arise from either DS or C-4-S. The dot that was digested with chondroitinase ACII should contain these disaccharides only from C-4-S. The dot that was digested with chondroitinase ABC should contain these disaccharides from both DS and C-4-S. Hence, if the sample contains both DS and C-4-S, the expectation is that the dot that was treated with chondroitinase ABC should contain more terminal 4-sulfated unsaturated disaccharides and, thus, be more intense than the dot that was treated with chondroitinase ACII. However, the reverse is observed, and there is no obvious explanation for this. One possibility is that this results from differences in the efficiencies of chondroitinase ACII and ABC toward co-polymers of dermatan sulfate and chondroitin sulfate. Chondroitinase ACII does not efficiently cleave such co-polymers. In contrast, dermatan sulfate-chondroitin sulfate co-polymers are efficiently cleaved by chondroitinase ABC, which digests both dermatan sulfate and chondroitin sulfate. It may be that the dot that was treated with chondroitinase ABC is less intense because the digestion was overly extensive relative to the dot that was treated with chondroitinase ACII and that this resulted in the presence of less terminal 4-sulfated unsaturated disaccharide and less 2B6 reactivity. Perhaps a shorter enzyme treatment time of the dots or a lower enzyme amount would result in more intense 2B6 reactivity in the DS + C-4-S dot relative to the C-4-S dot.

In conclusion, we have shown that the organic matrix of the red claw crayfish gastrolith contains proteoglycans that have dermatan sulfate, chondroitin-4-sulfate, chondroitin-6-sulfate, and keratan sulfate glycosaminoglycans. These glycosaminoglycans are likely to be not all on the same core protein, but, for at least some of the glycosaminoglycans, present in different proteoglycans. These macromolecules are closely associated with the mineral phase of the gastrolith and are easily removed by decalcification procedures. There are also some indications that the epithelial secretion of some of these molecules is temporally regulated during the molting cycle, but its gene regulation needs further investigation. Even if sulfate groups have been already thought to be involved in the chelation of calcium ions similarly to phosphate and carboxylate groups, the precise role of these

sulfated macromolecules in calcification and stabilization of the amorphous calcium carbonate phase of gastroliths is still to be established.

ACKNOWLEDGEMENTS

The work has been financially supported by the Ministry of Foreign Affairs (France) and CONICYT (Chile) through the ECOS-Sud/CONICYT Project C07B02 and through FONDAP 11980002. The work of G.L. was also supported by an ANR budget (ACCRO-EARTH, ref. BLAN06-2_159971) granted for the period 2007-2010 and by INSU-CNRS within the INTERRVIE project granted in 2010.

REFERENCES

Addadi, L., S. Raz, and S. Weiner. 2003. Taking advantage of disorder: amorphous calcium carbonate and its roles in biomineralization. Advanced Materials 15: 959-970.

Aizenberg, J., L. Addadi, S. Weiner, and G. Lambert. 1996. Stabilization of amorphous calcium carbonate by specialized macromolecules in biological and synthetic precipitates. Advanced Materials 8: 222-226.

———, G. Lambert, S. Weiner, and L. Addadi. 2002. Factors involved in the formation of amorphous and crystalline calcium carbonate: a study of an ascidian skeleton. Journal of American Chemical Society 124: 32-39.

———, J. Hanson, M. Ilan, L. Leiserowitz, T. F. Koetzle, L. Addadi, and S. Weiner. 1995. Morphogenesis of calcitic sponge spicules: a role of specialized proteins interacting with growing crystals. Federation of American Societies for Experimental Biology Journal 9: 262-268.

Ajikumar, P. K., L. G. Wong, G. Subramanyam, R. Lakshminarayanan, and S. Valiyaveettil. 2005. Synthesis and characterization of monodispersed spheres of amorphous calcium carbonate and calcite spherules. Crystal Growth Design 5: 1129-1134.

Akiva-Tal, A., S. Kabaya, Y. S. Balazs, L. Glazer, A. Berman, A. Sagi, and A. Schmidt. 2011. In situ molecular NMR picture of bioavailable calcium stabilized as amorphous $CaCO_3$ biomineral in crayfish gastroliths. Proceedings of the National Academy of Sciences USA 108: 14763-14768.

Albeck, S., L. Addadi, and S. Weiner. 1996. Regulation of calcite crystal morphology by intracrystalline acidic proteins and glycoproteins. Connective Tissue Research 35: 365-370.

Arias, J. L., and M. S. Fernández. 2003. Biomimetic processes through the study of mineralized shells. Material Characterization 50: 189-195.

———, and ———. 2007. Biomineralization: From Paleontology to Materials Science. Editorial Universitaria, Santiago, Chile.

———, and ———. 2008. Polysaccharides and proteoglycans in calcium carbonate-based biomineralization. Chemical Reviews 108: 4475-4482.

———, K. Mann, Y. Nys, J. M. García-Ruiz, and M. S. Fernández. 2007. Eggshell growth and matrix macromolecules, pp. 309-327. In, E. Bauerlein (ed.), Handbook of Biomineralization. Vol. 1. Wiley-VCH, Weinheim, Germany.

———, D. A. Carrino, M. S. Fernández, J. P. Rodriguez, J. E. Dennis, and A. I. Caplan. 1992. Partial biochemical and immunochemical characterization of avian eggshell extracellular matrices. Archives of Biochemistry and Biophysics 298: 293-302.

———, A. Neira-Carrillo, J. I. Arias, C. Escobar, M. Bodero, M. David, and M. S. Fernández. 2004. Sulfated polymers in biological mineralization: a plausible source for bio-inspired engineering. Journal of Material Chemistry 14: 2154-2160.

Bauerlein, E. 2000. Biomineralization. Wiley-VCH, Weinheim.

———. 2007. Handbook of Biomineralization. Wiley-VCH, Weinheim.

Becker, A., U. Bismayer, M. Epple, H. Fabritius, B. Hasse, J. Shi, and A. Ziegler. 2003. Structural characterization of X-ray amorphous calcium carbonate (ACC) in sternal deposits of the crustacean *Porcellio scaber*. Dalton Transactions: 551-555.

Belcher, A. M., X. H. Wu, R. J. Christensen, P. K. Hasma, G. D. Stucky, and D. E. Morse. 1996. Control of crystal phase switching and orientation by soluble mollusk-shell proteins. Nature 381: 56-58.

Bentov, S., S. Weil, L. Glazer, A. Sagi, and A. Berman. 2010. Stabilization of amorphous calcium carbonate by phosphate rich organic matrix proteins and by single phosphoamino acids. Journal of Structural Biology 171: 207-215.

Bülow, H. E., and O. Hobert. 2006. The molecular diversity of glycosaminoglycans shaped animal development. Annual Review of Cell and Developmental Biology 22: 375-407.

Carrino, D. A., J. L. Arias, and A. I. Caplan. 1991. A spectrophotometric modification of a sensitive densitometric Safranin O assay for glycosaminoglycans. Biochemistry International 24: 485-495.

———, J. P. Rodriguez, and A. I. Caplan. 1997. Dermatan sulfate proteoglycans from the mineralized matrix of the avian eggshell. Connective Tissue Research 36: 175-193.

———, J. E. Dennis, R. F. Drushel, S. E. Haynesworth, and A. I. Caplan. 1994. Identity of the core proteins of the large chondroitin sulfate proteoglycans synthesized by skeletal muscle and prechondrogenic mesenchyme. Biochemical Journal 298: 51-60.

Casu, B. 1985. Structure and biological activity of heparin. Advanced Carbohydrate Chemistry and Biochemistry 43: 51-134.

Caterson, B., T. Calabro, and A. Hampton. 1987. Monoclonal antibodies as probes for elucidating proteoglycan structure and function, pp. 1-26. In, T. N. Wright and R. P. Mecham (eds.), Biology of Proteoglycans. Academic Press, London.

———, J. E. Christner, J. R. Baker, and J. R. Couchman. 1985. Production and characterization of monoclonal antibodies directed against connective tissue proteoglycans. Federation Proceedings of the Federation of the American Societies of Experimental Biology 44: 386-393.

Díaz-Dosque, M., P. Aranda, M. Darder, J. Retuert, M. Yazdani-Pedram, J. L. Arias, and E. Ruiz-Hitzky. 2008. Use of biopolymers as oriented supports for the stabilization of different polymorphs of biomineralized calcium carbonate with complex shape. Journal of Crystal Growth 310: 5331-5340.

Ehrlich, H. 2010. Chitin and collagen as universal and alternative templates in biomineralization. International Geological Review 52: 661-669.

Falini, G., S. Albeck, S. Weiner, and L. Addadi. 1996. Control of aragonite or calcite polymorphism by mollusk shell macromolecules. Science 271: 67-69.

Fernández, M. S., M. Araya, and J. L. Arias. 1997. Eggshells are shaped by a precise spatio-temporal arrangement of sequentially deposited macromolecules. Matrix Biology 16: 13-20.

———, A. Moya, L. López, and J. L. Arias. 2001. Secretion pattern, ultrastructural localization and function of extracellular matrix molecules involved in eggshell formation. Matrix Biology 19: 793-803.

———, I. Vergara, A. Oyarzun, J. L. Arias, R. Rodriguez, J. P. Wiff, V. M. Fuenzalida, and J. L. Arias. 2002. Extracellular matrix molecules involved in barnacle's shell mineralization, pp. 1-9. In, J. Aizenberg, J. McKittrick, and C. Orme (eds.), Biological and Biomimetic Materials – Properties to Function. Material Research Society Symposium Proceedings. Vol. 724. Warrendale, PA.

Funderburgh, J. L. 2000. Keratan sulfate: structure, biosynthesis, and function. Glycobiology 10: 951-958.

Gago-Duport, L., M. J. I. Briones, J. B. Rodríguez, and B. Covelo. 2008. Amorphous calcium carbonate biomineralization in the earthworm's calciferous gland: pathways to the formation of crystalline phases. Journal of Structural Biology 162: 422-435.

Glazer, L., A. Shechter, M. Tom, Y. Yudkovski, S. Well, E. D. Aflalo, R. R. Pamuru, I. Khalaila, S. Bentov, A. Berman, and A. Sagi. 2010. A protein involved in the assembly of an extracellular calcium storage matrix. Journal of Biological Chemistry 285: 12831-12839.

Huckerby, T. N. 2002. The keratan sulphates: structural investigations using NMR spectroscopy. Progress in Nuclear Magnetic Resonance Spectroscopy 40: 35-110.

Iozzo, R. V. 1998. Matrix proteoglycans: from molecular design to cellular function. Annual Review of Biochemistry 67: 609-659.

Ishii, K., N. Tsutui, T. Watanabe, T. Yanagisawa, and H. Nagasawa. 1998. Solubilization and chemical characterization of an insoluble matrix protein in the gastroliths of a crayfish, *Procambarus clarkii*. Bioscience, Biotechnology and Biochemistry 62: 291-296.

Lee, H. S., T. H. Ha, and K. Kim. 2005. Fabrication of unusually stable amorphous calcium carbonate in an ethanol medium. Materials Chemistry and Physics 93: 76-382.

Loste, E., R. M. Wilson, R. Seshadri, and F. C. Meldrum. 2003. The role of magnesium in stabilising amorphous calcium carbonate and controlling calcite morphologies. Journal of Crystal Growth 254: 206-218.

Lowenstam, H. A., and S. Weiner. 1989. On Biomineralization. Oxford University Press, Oxford.

Luquet, G., and F. Marin. 2004. Biomineralizations in crustacean: storage strategies. Comptes Rendus Palevol 3: 515-534.

———, M. S. Fernández, J. M. Navarrete, J. L. Arias, N. Guichard, B. Marie, and F. Marin. 2007. Biochemical characterization of the soluble organic matrix of gastroliths from decapods, pp. 319-328. In, J. L. Arias

and M. S. Fernández (eds.), Biomineralization, from Paleontology to Materials Science. Editorial Universitaria, Santiago, Chile.

Mann, S. 2001. Biomineralization. Oxford University Press, Oxford.

———, P. Behrens, and E. Bauerlein. 2007. Handbook of Biomineralization. Biomimetic and Bioinspired Chemistry. Wiley-VCH, Weinheim.

———, J. Webb, and R. J. P. Williams. 1989. Biomineralization. VCH, Weinheim.

Mehmet, H., P. Sculder, P. W. Tang, E. F. Hounsell, B. Caterson, and T. Feizi. 1986. The antigenic determinants recognized by three monoclonal antibodies to keratan sulphate involve sulphated hepta or larger oligosaccharides of the poly(N-acetylgalactosamine) series. European Journal of Biochemistry 157: 385-391.

Morse, A. 1945. Formic acid-sodium citrate decalcification and butyl alcohol dehydration of teeth and bone for sectioning in paraffin. Journal of Dental Research 24: 143-153.

Nakatsuji, T., H. Keino, K. Tamura, S. Yoshimura, T. Kawakami, S. Aimoto, and H. Sonobe. 2000. Changes in the amounts of the molt-inhibiting hormone in sinus glands during the molt cycle of the American crayfish, *Procambarus clarkii*. Zoological Science 17: 1129-1136.

Ndao, M., E. Keene, F. F. Amos, G. Rewari, C. B. Ponce, L. Estroff, and J. S. Evans. 2010. Intrinsically disordered mollusk shell prismatic protein that modulates calcium carbonate crystal growth. Biomacromolecules 11: 2539-2544.

Neira-Carrillo, A., M. Yazdani-Pedram, J. Retuert, M. Diaz-Dosque, S. Gallois, and J. L. Arias. 2005. Selective crystallization of calcium salts by poly(acrylate)-grafted chitosan. Journal of Colloidal Interface Science 286: 131-141.

Nys, Y., M. T. Hincke, J. L. Arias, J. M. García-Ruiz, and S. E. Solomon. 1999. Avian eggshell mineralization. Poultry Avian Biology Review 10: 142-166.

Raz, S., S. Weiner, and L. Addadi. 2000. Formation of high-magnesian calcites via an amorphous phase: possible biological implications. Advanced Materials 12: 38-42.

———, O. Testeniere, A. Hecker, S. Weiner, and G. Luquet. 2002. Stable amorphous calcium carbonate is the main components of the calcium storage structures of the crustacean *Orchestia cavimana*. Biological Bulletin 203: 269-274.

Rodríguez-Navarro, A., C. Cabral de Melo, N. Batista, N. Morimoto, P. Alvarez-Lloret, M. Ortega-Huertas, V. M. Fuenzalida, J. I. Arias, J. P. Wiff, and J. L. Arias. 2006. Microstructure and crystallographic-texture of giant barnacle (*Austromegabalanus psittacus*) shell. Journal of Structural Biology 156: 355-362.

Sato, A., S. Nagasaka, K. Furihata, S. Nagata, I. Arai, K. Saruwatari, T. Kogure, S. Sakuda, and H. Nagasawa. 2011. Glycolytic intermediates induce amorphous calcium carbonate formation in crustaceans. Nature Chemical Biology 7: 197-199.

Shechter, A., A. Berman, A. Singer, A. Freiman, M. Grinstein, J. Erez, E. D. Aflalo, and A. Sagi. 2008a. Reciprocal changes in calcification of the gastrolith and cuticle during the molt cycle of the red claw crayfish *Cherax quadricarinatus*. Biological Bulletin 214: 122-134.

———, L. Glazer, S. Cheled, E. Mor, S. Weil, A. Berman, S. Bentov, E. D. Aflalo, I. Khalaila, and A. Sagi. 2008b. A gastrolith protein serving a dual role in the formation of an amorphous mineral containing extracellular matrix. Proceedings of the National Academy of Sciences 105: 7129-7134.

Simkiss, K., and K. M. Wilbur. 1989. Biomineralization. Academic Press, San Diego.

Smith, B. L., T. E. Schäffer, M. Viani, J. B. Thompson, N. A. Frederick, J. Kindt, A. M. Belcher, G. D. Stucky, and D. E. Morse. 1999. Molecular mechanistic origin of the toughness of natural adhesives, fibres and composites. Nature 399: 761-763.

Sugahara, K., and H. Kitagawa. 2000. Recent advances in the study of the biosynthesis and functions of sulfated glycosaminoglycans. Current Opinion on Structural Biology 10: 518-527.

Takagi, Y., K. Ishii, N. Ozaki, and H. Nagasawa. 2000. Immunolocalization of gastrolith matrix protein (GAMP) in the gastroliths and exoskeleton of crayfish, *Procambarus clarkia*. Zoological Sciences 17: 179-184.

Testeniere, O., A. Hecker, S. Le Gurun, B. Quennedey, F. Graf, and G. Luquet. 2002. Characterization and spatiotemporal expression of orchestin, a gene encoding an ecdysone-inducible protein from a crustacean organic matrix. Biochemical Journal 361: 327-335.

Thormann, E., H. Mizuno, K. Jansson, N. Hedin, M. S. Fernández, J. L. Arias, M. W. Rutland, R. Krishna Pai, and L. Bergström. In press. Embedded proteins and sacrificial bonds provide the strong adhesive properties of gastroliths. Nanoscale.

Travis, D. F. 1960. The deposition of skeletal structures in the crustacea. I. The histology of the gastrolith skeletal tissue complex and the gastrolith in the crayfish, *Orconectes* (*Cambarus*) *virilis* Hagen – Decapoda. Biological Bulletin 18: 137-149.

———. 1963. Structural features of mineralization from tissue to macromolecular levels of organization in the decapod crustacea. Annals of the New York Academy of Science 109: 177-245.

Tsutsui, N., K. Ishii, Y. Takagi, T. Watanabe, and H. Nagasawa. 1999. Cloning and expression of a cDNA encoding an insoluble matrix protein in the gastroliths of a crayfish, *Procambarus clarkii*. Zoological Sciences 16: 619-628.

Volkmer, D., M. Harms, L. Gower, and A. Ziegler. 2005. Morphosynthesis of nacre-type laminated $CaCO_3$ thin films and coatings. Angewandte Chemie International Edition 44: 639-644.

Weiner, S., and L. Addadi. 1997. Design strategies in mineralized biological materials. Journal of Materials Chemistry 7: 689-702.

Xu, A.-W., Q. Yu, W.-F. Dong, M. Antonietti, and H. Cölfen. 2005. Stable amorphous $CaCO_3$ microparticles with hollow spherical superstructures stabilized by phytic acid. Advanced Materials 17: 2217-2221.

Yanagishita, M., and V. C. Hascall. 1984. Proteoglycans synthesized by rat ovarian granulosa cells in culture. Isolation, fractionation, and characterization of proteoglycans associated with the cell layer. Journal of Biological Chemistry 259: 10260-10269.

Yudkovski, Y., L. Glazer, A. Shechter, R. Reinhardt, V. Chalifa-Caspi, A. Sagi, and M. Tom. 2010. Multi-transcript expression patterns in the gastrolith disk and the hypodermis of the crayfish *Cherax quadricarinatus* at premolt. Comparative Biochemistry and Physiology Part D Genomics Proteomics 5: 171-177.

RECEIVED: 13 January 2012.
ACCEPTED: 1 May 2012.